

Extent of UV Curing in Highly Loaded Systems for Direct Ink

Writing

Zachary Kenneth Adams

Submitted 1 May 2021

Table Of Contents

Title Page.....	1
Table of Contents.....	2
Abstract.....	3
Introduction.....	3
Materials and Methods.....	7
Results.....	15
Discussion.....	17
Conclusion.....	19
References.....	21
Appendix A (GCODE)	23
Appendix B (MATLAB Code)	28

Abstract

This study investigates the solidification of material 3D-printed via direct ink writing. This material, consisting of monomers, a photoinitiator and silicon microspheres was extruded onto a printing bed. The material was then irradiated with ultraviolet light to polymerize the monomers. Curing time and thickness of the material were varied in order to determine their effect on the solidification process. Quantification of the extent of cure was done using Fourier transform infrared spectroscopy. The data collected show that the degree of conversion tends to decrease as curing time decreases, but the data is inconclusive as to the specific relationship between time and degree of cure. However, due to a combination of a long method development process and the coronavirus pandemic, work on this project was halted before this trend could be definitely proven.

Introduction

Direct ink writing (DIW) is a promising method of additive manufacturing, or 3D printing in this instance. Similar to fused deposition modelling (FDM), the most popular method of 3D printing, it can be used to print parts quickly and with complex geometries. With DIW, engineers can utilize a diverse range of material types, allowing for an even greater range of customization, especially for printing suspensions. Instead of heating up a filament-based polymeric material past its glass transition temperature like in FDM, DIW extrudes shear-thinning material out of a syringe onto the printing bed. This semi-liquid extrusion is what enables the customizability of DIW. There are a large number of factors that affect the flow of material through the nozzle, which, when properly understood and controlled, can give a high deal of control over the printing process. Post-extrusion, the material can be solidified using one of the two following methods: solvent evaporation or post extrusion polymerization, depending on the type of ink used. Polymerization would be initiated by heat or ultraviolet (UV) radiation. Since the material must flow well in order to be printed, the material's rheological, or fluid-like, properties have to be carefully engineered to ensure quality printing.

One popular method for post-extrusion solidification uses a polymerization reaction that is initiated by UV radiation. Referred to as UV curing, this process involves passing an ultraviolet light source emitting a wavelength between 10nm and 400nm over the extruded material (common wavelengths for UV LEDs include 368, 385 and 405nm). During the process,

monomer species in the extruded material react to form highly crosslinked polymers. Photosensitive molecules have to be added to the material in order for this method to work. The high intensity light causes these photosensitive molecules, also known as photoinitiators, to form highly reactive radical species, which start the polymerization reaction that solidifies the extruded material.

The material used in DIW consists of a mixture of liquids and particulate solids that form a solid, hardened part after printing and curing. The liquid portion is referred to as the ‘resin’, while the solid portion is referred to as ‘the solids’. The solids give the material its shape and structure and can provide advanced functionality, while the liquid portion allows it to flow before hardening. Post-hardening, the material is a composite, with its properties depending on the makeup of the solids and resin. For performing fundamental studies, hollow silicon dioxide spheres (hSiO_2), with a diameter of $10\mu\text{m}$, are an ideal choice for the solids as they are inexpensive, nonreactive and their regular geometry allows for a relatively ordered microstructure.

A popular resin system to use for UV curing is a mixture of bisphenol a-glycidyl methacrylate (BisGMA) and triethylene glycerol dimethacrylate (TEGDMA) monomers with their structure shown in Fig. 1. These compounds are commonly used in modern dental fillings. As purchased, both monomers are liquid, but BisGMA has a viscosity of 1200 Pa s [1] and TEGDMA has a viscosity of 0.011 Pa s [2]. Due to its high viscosity, BisGMA has to be mixed with a lower viscosity liquid in order to produce a usable solution. This is one of the primary reasons BisGMA is combined with TEGDMA. BisGMA has advantageous physical properties such as high strength, fast cure time and low shrinkage due to curing. These properties, however, are lost as the amount of TEGDMA is increased [3]. The reactivity of the resin, however, is increased as TEGDMA is added to the mixture, up until a 1:1 molar ratio is reached, maximizing the reactivity of the system [4].

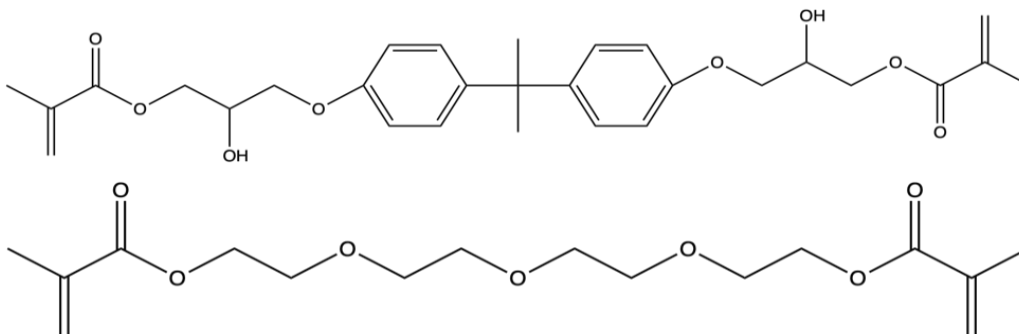


Fig. 1. The BisGMA (top) and TEGDMA (bottom) monomers.

The extent to which the material cures is known as the degree of cure (DC), and is measured as a percentage. Two methods are widely used in order to characterize the DC of UV curable materials: Fourier transform infrared spectroscopy (FTIR) and differential scanning calorimetry (DSC). FTIR is the most widely used method [5] - [13] though DSC [14], [15] has been shown to be valuable. FTIR can record, among other information, the absorbance of infrared radiation at a range of possible wavenumbers (inverse wavelength). Peaks on the graph are specific to certain chemical bonds. FTIR, therefore, can be a powerful method for characterization in this application because it can show peaks that are unique only to the unpolymerized monomers [9]. FTIR is limited, however, in that the attenuated total reflection (ATR) method, which must be used to characterize solid films and powders, cannot analyze more than several hundred micrometers into the material [16], making it difficult to receive bulk information for larger pieces. The second possible characterization method, DSC applies a known amount of thermal energy to a sample and records the corresponding temperature rise in the loaded material. As the sample's DC increases, the temperature rise from the heat flow decreases, allowing the relative DC to be determined. Due to the bulk nature of the samples for DSC, it is easier to get averaged information on the total sample using this method, as the heat flow through the material is not dependent on its size [17].

An alternative method to FTIR and DSC is via the use of fluorophores. In response to plane polarized radiation, fluorophores rotate a specific amount. This rotation can be determined by measuring the fluorescence of the material at specific angles. The amount of rotation is dependent on the free space in the material, which is directly related to its DC [18]. These fluorophores have to be incorporated into the material being investigated and expensive microscopy must be performed, which limits their use. An improvement on this method uses a

cheaper microscope, but it still retains the problems of the original, requiring an extensive optical setup [19]. This method is low-cost once the equipment and expertise is available and could be beneficial in both a laboratory and industrial setting. The setup, however, is not the most ideal when there is easy access to FTIR and DSC machines, as those are relatively easier to implement.

The DC of a UV curable material is dependent on many variables: the intensity of the UV light, the wavelength of the UV light, the amount of time the UV light was applied to the material, the thickness of the material, the identity of the material's components, etc. Thickness is a major factor affecting DC since the material used, primarily the hSiO_2 , is UV opaque, meaning that the solids in the material absorb, reflect and/or scatter the UV light needed to cure the resin. The DC at increasing depths is likely to decrease as fewer photons will be available to initiate the polymerization process. Irradiation time is another important factor as the curing reaction is not an instantaneous process. Without UV light actively shining, the polymerization reaction quickly terminates, as reactive species propagating the reaction quickly degrade. This thesis aims to investigate the relationship between DC, the depth into the material, and irradiation time.

Curing time has been established by previous work to be a variable with a large impact on DC [5], [6], [7], [8], [12], [13], [14]. The DC versus time profile follows a seemingly logarithmic curve. A significant portion of the curing for a UV cured material occurs within the first ten seconds [12]. At longer timescales, the DC changes slowly with time, eventually reaching an asymptotic value. For methacrylate based systems, this value is around 70% [5]. Once the irradiation stops, it has been found that the reaction continues at a much slower rate. Evaluating the DC of a UV cure material 24 hours post-irradiation found that the DC increased by less than 5% [5].

Evaluating how the DC changes with depth into the material is much less established in the literature. Only a few papers have investigated the relationship between DC, time and depth [6], [7]. These papers have found that the DC does decrease with added depth, but they disagree on how much it changes. A paper in 1987 found that the percent of double bonds remaining (inversely proportional to DC) decreased sharply from 75% to 25% as the material increased in depth from 0.1 to 6 mm over 60 seconds of irradiation [7]. Another paper, published in 2013, only found significant changes in DC at 4mm and 6 mm for shorter time scales [6]. Both papers,

however, only evaluated the DC at irradiation time scales of 20s, 40s, and 60s, which is quite a small and limited scale even if it captures most of the material's curing. Although these papers studied commercially available materials, the resins were methacrylate based. Additionally, no work has been done as of yet in order to understand the relation between DC, time and depth for the particle/polymer composite material designed to be 3D-printed via DIW.

In this investigation, a method for determining the relationship between the DC of a part printed via DIW, curing time, and depth into the material is developed. The DC of 3D printed parts has not been analyzed using DSC as of yet, and there is minimal research on how depth affects DC, even in non-3D printed materials. A significant amount of work on this project was spent on developing this method, and trying to successfully implement ideas from several different papers. Throughout the course of the investigation, many parameters were changed, different curing speeds and light intensities were tried, all in service to produce reliable results. The parameter values listed in this paper are the values used in the most recent run of experiments.

Materials and Methods

Materials

The material used for printing in this investigation has three primary components: the resin, the solids, and the photoinitiator. The resin is a homogeneous mixture of two monomers: bisphenol A-glycidyl methacrylate (BisGMA) and triethylene glycol dimethacrylate (TEGDMA). The BisGMA was purchased from Sigma Aldrich (CAS: 1565-94-2) and the TEGDMA was purchased from the Tokyo Chemical Industry (CAS: 109-16-0). The TEGDMA is stabilized with no more than 5% Mequinol which serves as a polymerization inhibitor. Both chemicals were used as purchased, and were stored together in a dark cabinet, wrapped with tin foil to prevent UV exposure. It should be noted that the BisGMA was stored at room temperature, approximately 20°C, instead of the recommended 2-8°C.

The solids consist of hollow silicon dioxide microspheres. The spheres have diameters between 9µm and 13µm. The hollow microspheres were purchased from Sigma Aldrich (CAS: 65997-17-3) and used as purchased.

The photoinitiator for this material is 1-hydroxycyclohexyl phenyl ketone (commercially known as Irgacure 184). This chemical was purchased from Sigma Aldrich (CAS: 947-19-3) and

used as purchased. The container of photoinitiator was stored in a Secador brand desiccator to prevent exposure to water. This desiccator also advertises 99% UV light protection.

Preparing the printing material

This resin consists of BisGMA and TEGDMA in a 2:1 ratio, by mass, of BisGMA to TEGDMA. Approximately 50mL of the resin were made at a time. The BisGMA was measured out first using a spatula due to its high viscosity. The TEGDMA, with a much lower viscosity, was then measured out using a 10mL BD plastic syringe. After measuring, the two monomers were added together in a 100mL polypropylene FlackTek mixing cup. This cup was then covered in tin foil to prevent UV exposure and was placed on a shaker table overnight to ensure thorough mixing of the monomers.

The printing material compositions is as follows: the solids are 61.4% by volume and the resin makes up the remaining 38.6%. The photoinitiator is added as an additional 1 weight percent of the final mass of the material. 25mL of printing material were made at a time. The resin was measured out using a 10mL syringe, and was emptied into a 50mL polypropylene FlackTek mixing cup. The mass of hollow silicon dioxide microspheres to be added was calculated from the required volume percent of solids and the provided value for density, 1.1 g/cm³. The SiO₂ was measured out in a separate container so that the total mass of the material (resin + solids) could be determined for the addition of the photoinitiator. The photoinitiator was added to the resin and the container was placed on the shaker table for twenty minutes to dissolve. While on the shaker table, tin foil was placed over the container. With the photoinitiator fully incorporated, the solids were added to the resin by pouring the SiO₂ powder on top of the liquid resin and photoinitiator mixture. The container was sealed tight and covered in tin foil for the next step.

Now combined, the material needed to be mixed thoroughly, in order to make a homogenous mixture. A high speed mixer was used to combine the solids, resin and photoinitiator, and a FlackTek DAC 400.2-VAC was used throughout this investigation. At different times, the mixer was used with a syringe holder and 50mL cup holder. These were polyethylene inserts placed into the mixing drum to hold the container in place. The mixer is capable of mixing at speeds from 800 rpm to 2500rpm for any sample under 300g. In this investigation, the material was mixed at 1000rpm for 30 seconds and then at 1500 rpm for 2

minutes 30 seconds, a method optimized in previous work to keep the temperature rise from mixing under 10°C [20]. After mixing, the container was placed on a lab counter and the material was allowed to cool down to room temperature. The container was covered in tin foil at all times outside the mixer. When loaded in the mixer, the tin foil had to be removed for the container to fit in the inserts.

When the material was ready to use, it was carefully loaded into a 30mL BD plastic syringe that had been coated with a film intended to limit the UV exposure of the material within. The material was loaded by pulling the stopper off of the syringe and using a spatula to place all of the prepared material, approximately 25mL, in the syringe cavity. The stopper was put back in place with a bent paperclip in between the syringe wall and the stopper to create a small gap as can be seen in Fig. 2. The stopper was pushed down until the material started to extrude out the tip. The syringe tip was then capped and taken to the mixer. The syringe was spun for 1 minute at 1000rpm in order to remove trapped air bubbles that were entrained when loading the material into the syringe. When the spinning finished, the stopper of the syringe was pressed as firmly as possible. Air bubbles liberated from the material during spinning would exit the syringe through the gap created by the paperclip. Its job now complete, the paperclip was removed, and the syringe was wrapped with tinfoil in order to minimize UV exposure before being used.



Fig. 2. (left) loaded syringe with paperclip pre-mixing. (right) loaded syringe with paperclip post mixing.

3D Printer Configuration

The printer used in this investigation is a Hydra16A printer manufactured by Hyrel. This printer has many slots for a diverse range of heads to be attached. For this investigation, custom-built heads to hold 30mL BD syringes and a UV light were attached to the printer. The syringe holder, which will be referred to as the ‘printing head’ was installed in slot 1 and the UV light was installed in slot 3. The heads had to be installed in these positions due to the printing program. The printer has a spatial resolution of $6\mu\text{m}$ in the x/y axes, $1\mu\text{m}$ in the z axis and a spatial accuracy of $\pm 60\mu\text{m}$ in the x/y axes and $\pm 10\mu\text{m}$ in the z axis. The printer was controlled by a computer running the software Repetrel, and the print file was written in GCODE.

The GCODE used for this investigation can be found in Appendix A.

The printer bed is a large slab of aluminum with a plate of glass centered on the top. Attached with tape to the printer bed, this was used to provide a level surface to print upon. For each experiment in this investigation, a 3M plastic transparency sheet was taped down with its smooth side facing up. This gives a good surface for the adhesion of the printed material, and made cleaning up each experiment much easier. The setup can be seen in Fig. 3.

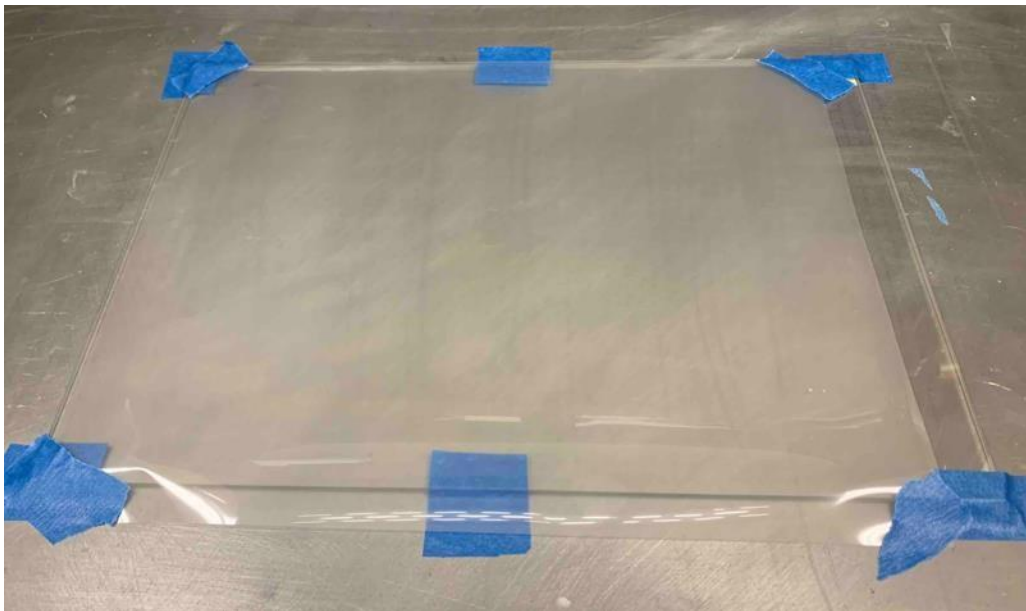


Fig. 3. The printer bed with glass plate and plastic transparency sheet.

Setting up the Printer

The syringe was installed in the printing head by manually adjusting the motor so that the syringe would slide into its place. The setup of the printer is shown in Fig. 4. The syringe cap had to be removed in order for the syringe to be inserted, but was placed back on after the syringe was mounted. Just prior to printing, the cap was removed and replaced with a 10mm diameter syringe tip. With the tip on, the printer's z-height was calibrated. This was done by moving a piece of paper underneath the tip and decreasing the distance from the tip to the printer bed until there was noticeable resistance on the movement of the paper. The program was then loaded up and the printer was ready to go.



Fig. 4. The 3D printer fully set up for the experiment. The print head with syringe loaded is on the left and the UV light is to the right.

Printing and Curing the Material

Each printing experiment could begin once the syringe was inserted and the printer was configured. The printing began as soon as the 'start' button on the computer was pressed. Following the program, the printer extruded material in 2.5 parallel lines before printing a line perpendicular to the previous lines in the center of the bed, as shown in Fig. 5. This perpendicular segment will be referred to as the 'test line', while the parallel lines are the

‘priming lines’. In order to evaluate how the depth into the sample affects its curing, the number of layers printed had to be varied. Prints with increasing z-heights were done by printing the first layer normally, and then printing the extra layers on the test line. This would prevent the printing of additional layers from taking too long, which could cause the layers to flow and flatten out. All of the printing was done at a speed of 600mm/min to ensure a quality print. Once the printer finished, the bed dropped, and the program paused. The syringe tip had to be screwed off and the syringe cap had to be screwed on before the program could continue, to prevent material from leaking out the syringe while curing.

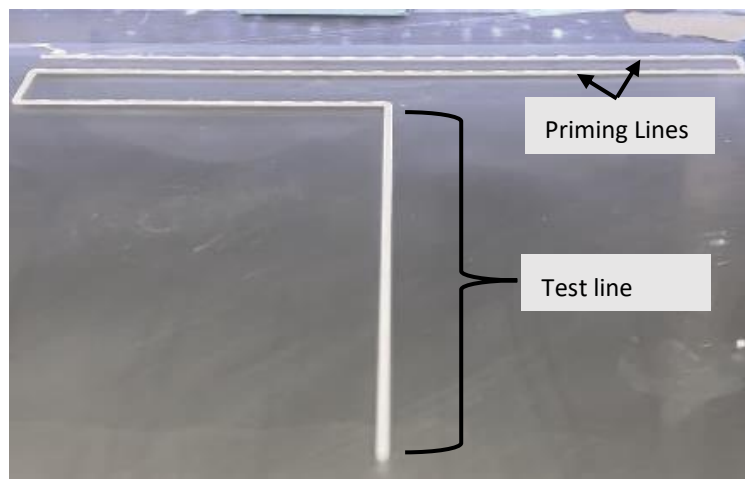


Fig. 5. A top down view of the result of the 3D printing program used in this experiment. The ‘test’ line can be seen front and center while the ‘priming’ lines can be seen towards the back.

When the program continued, the UV light powered up and the printer head followed the same path as the printing stage. The UV light had its power set to 50% for all the experiments in this investigation. A small offset for the printing head was used so that the center of the UV light was in the center of the printed material. The speed of the curing head was set to 1000mm/min for the priming lines while the speed was varied over the test line. The speed was varied in order to expose the material to UV light for different amounts of time. In this investigation, The speeds used were: 100mm/min, 1000mm/min, 5000mm/min, 7500mm/min, and 10000mm/min. For all prints, including those with increased z-heights, the UV lamp was kept at a constant height of 10 mm over the printing bed.

After the UV light finished tracing the printed material, the program paused again. This gave time for the now cured lines to be removed from the printer bed. The test line was removed first, cut into pieces approximately 5cm long and stored in an amber vial. The priming lines were all discarded.

With the printer bed now clean, this entire printing process could be restarted. Before continuing the program, the cap was taken off and the syringe tip was put back on. The program was then resumed, and the printer started to print again. The printing followed the same parameters as before. When the printing finished, the UV curing occurred in the same way as before, but at a different speed over the test line. This procedure continued 3 more times, all at the same z-height, but with different curing speeds.

Measuring DC

Directly after the printing program finished, all of the amber vials were loaded onto a tray and carried to a separate lab for FTIR measurement. FTIR analysis was done on a Shimadzu Prestige 21 FT-IR spectrophotometer. This machine supports a maximum resolution of 0.50cm^{-1} and a signal to noise ratio of 40.000/1. The experiments were run using an attenuated total reflection (ATR) setup which uses a sapphire crystal. The machine was controlled by a computer running LabSolutions IR software.

Before loading any materials, a background scan was first conducted. The background scan and all sample runs were conducted with the following settings: Happ-Genzel apodization, 1cm^{-1} resolution, 50 scans per run, and a range of $1500\text{-}1800\text{cm}^{-1}$. The test ran for approximately 4 minutes after which the material in the machine was cleaned out and the machine was prepared to test again. 5 samples were tested from each of the amber vials brought to the lab. Additionally, leftover material from the syringe was also analyzed to establish a baseline. After testing, the files were exported as a text file and taken from the computer using a USB flash drive.

Quantification of degree of cure

The data collected from the FTIR was imported into MATLAB for analysis. The code can be found in Appendix B. The data were then filtered using Savitzky-Golay Filtering with an order of 3 and frame length of 31. Normalization was then performed by dividing the entire dataset by the absorbance value of the peak at 1720 cm^{-1} .

With the data normalized, the DC could be calculated. This value is directly related to the molar ratio between aliphatic and aromatic bonds. The aliphatic bonds correspond to the peak at 1640 cm^{-1} , while the aromatic bonds correspond to peaks at 1608 cm^{-1} and 1582 cm^{-1} . To calculate the molar ratio between these peaks, two baselines were drawn: one from the base of the peak at 1637 cm^{-1} to the base of the peak at 1582 cm^{-1} , and one drawn underneath both bases of the peak at 1582 cm^{-1} . The molar ratio, χ , was calculated as the peak height of the 1637 cm^{-1} peak divided by the peak at 1582 cm^{-1}

$$\chi_i = \frac{P_{1637}}{P_{1582}} \quad (1)$$

Where P_{1637} and P_{1582} are the peak heights at 1637 cm^{-1} and 1582 cm^{-1} , respectively. The DC of each sample was then calculated using:

$$\text{DC}_i = \left(1 - \frac{\chi_i}{\chi_{\text{uncured}}}\right) \quad (2)$$

The variable, χ_{uncured} , is the molar ratio for the material that is completely uncured.

Results

A sample IR spectrum can be seen in Fig. 6. The data for this sample were collected on 3 March 2020, and printed with a layer height of 1mm. Figure 6 is from the first IR run of the material printed at 100mm/min. In the range of 1780 cm^{-1} to 1560 cm^{-1} , four distinct peaks are visible. The peak at 1637 cm^{-1} is due to aliphatic bonds in the uncured material and the peak at 1582 cm^{-1} is due to aromatic bonds.

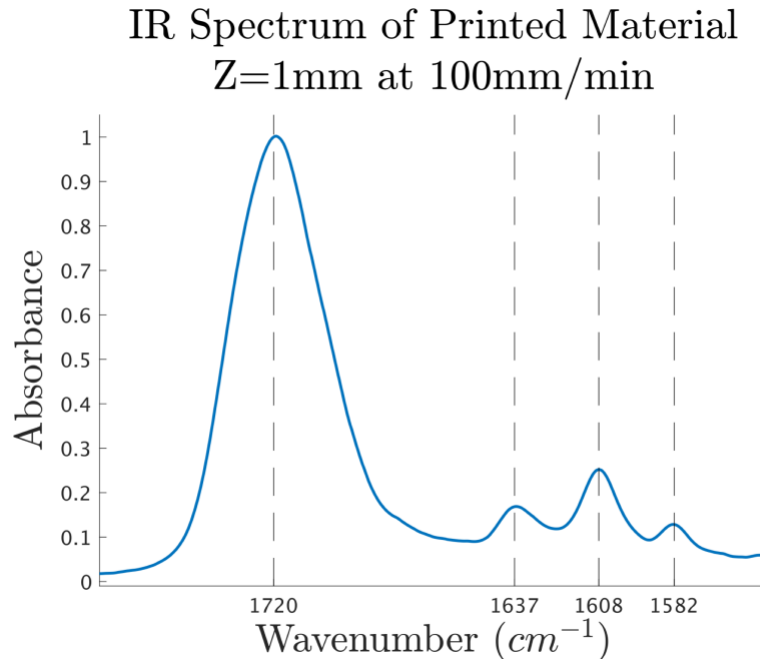


Fig. 6. The IR spectra of the 3D printed material with a thickness of 1mm that was cured at 1.6667×10^{-3} m/s.

This plot is from the first run at this printing speed.

For a printing thickness of 1mm, there were two experiments that produced usable data. These sets of data were collected on 3 March 2020 and 6 March 2020. Using Equation (1), the molar ratios were calculated from the heights of the peaks at 1637 cm^{-1} and 1582 cm^{-1} . The mean molar ratio and standard deviation for each printing speed are shown by printing date in Table 1. The mean molar ratio generally increases as printing speed increases, but the data has high variation, as evidenced by the standard deviations.

TABLE I
Molar Ratios of Samples Printed with 1mm Thickness

Curing Speed (mm/min)	3 March 2020		6 March 2020	
	Mean	Standard Deviation	Mean	Standard Deviation
100	2.052	0.419	2.290	0.187
1000	2.587	0.217	4.076	0.664
5000	3.621	0.228	5.460	0.398
7500	3.979	0.108	5.319	0.198
10000	4.969	0.343	5.573	0.318
Uncured	5.289	0.366	5.720	0.994

Using Equation (2), the molar ratios were converted into DCs. Fig. 7 shows a plot of DC versus the curing speed by date at a thickness of 1mm. The plotted data points are the mean of the DC for each curing speed, and the error bars are ± 2 standard deviations. The value plotted at 20000 mm/min was not a curing speed in this experiment. Instead, this is an arbitrary value to plot the DC values for uncured material. Similar to the molar ratios, the DC does appear to decrease as curing speed increases, but has a similar issue with high variability.

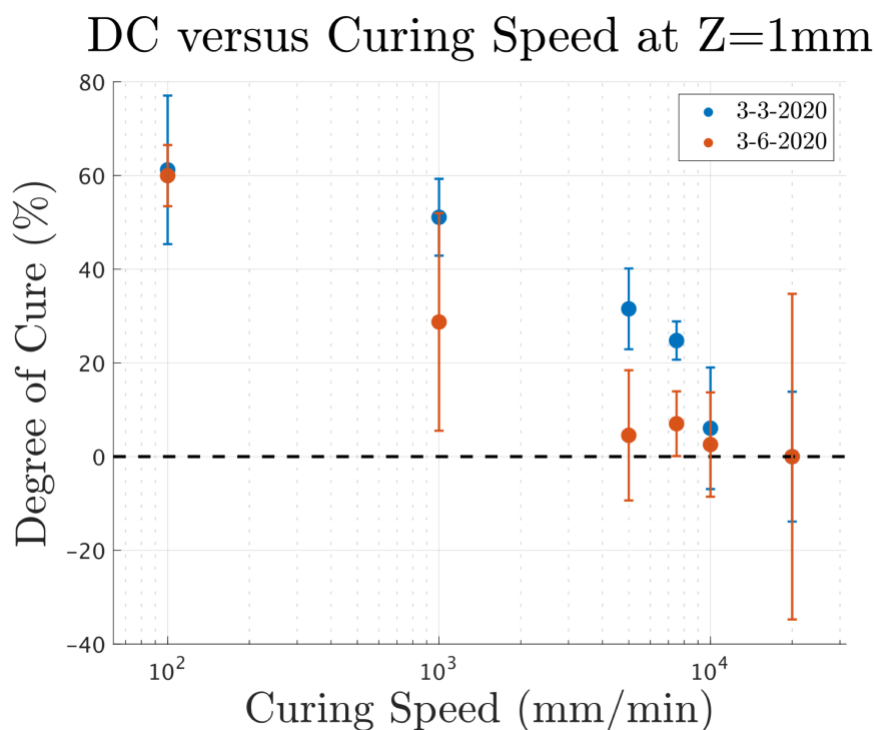


Fig. 7. The degree of conversion of the printed material versus curing speed in millimeters per minute. The value at 20000mm/min was not a curing speed used in the experiment, but is where the ‘Uncured’ values were plotted.

Due to the pandemic, undergraduate students were sent home after March 12th, 2020, and campus was closed until the following fall semester. This research lab was closed to undergraduate students through Jan 2021 with extremely restricted access after that, so further data was not able to be collected and analyzed.

Discussion

The collection of the FTIR spectra in this experiment proceeded with minimal difficulty. Aside from a minor amount of peak splitting, the spectra were decently smooth. The peak splitting was remedied with the filtering done in MATLAB. There was also a small amount of shifting, but these differences were insignificant. The data was quantified by a relative method, so any shift or baseline difference in the absorbance spectra would affect all the peaks similarly, not affecting the calculated molar ratios.

The trends in the molar ratios and DC versus curing speed are the same, as the DC is proportional to the molar ratio. As can be seen in Figure 7, there is a general downward trend in the DC vs. curing speed data. For the 3 March 2020 data, the DC for curing at lower speeds is

significantly different than the DC at higher speeds. A t-test performed to assess this claim returned a p-value of <0.01 . The 6 March 2020 data, decreases similarly, but the only data point that shows any significant difference is the DC at a printing speed of 100mm/min, which is further corroborated with a p-value of <0.01 when a t-test was performed. All the other data points are within each other's error bars. Also, between the two different dates, the same printing speeds produced different distributions of DCs. Sometimes the DCs for a single curing speed were wildly different between the two dates, as can be seen for 5000 mm/min.

The trend of decreasing DC with increasing curing speed is to be expected, as it makes intuitive sense that polymerization reactions with time for energy input will not reach the same extent of reaction in the same time. Despite this, the exact relationship beyond the general negative trend cannot be known. The incredibly high variance, as evidenced by the overlapping error bars in Figure 2 and the large standard deviations in Table 1 prevent any real conclusions being drawn from this data.

Variance in these data could be due to several different causes. One could be that there is a significant change in DC as the curing speed increases, but enough time passes between curing and measuring that post-irradiation curing becomes significant. If this happens, the DC of each sample will likely increase, but not proportionally to the amount of radiation it initially received. Another possibility could be that the peaks measured from the FTIR spectra are slightly off due to differences in loading. An FTIR spectra in an ATR setup is dependent on a wide range of factors, but the only factors that can possibly change when loading different samples is the area of contact with the ATR crystal and the efficiency of this contact. Care was taken during sample loading to only use pieces of material longer than the diameter of the ATR crystal, but the width of the material was less than the diameter. That means that most of the crystal is obscured, but variations in line width from printing may cause slightly different amounts of area of the crystal to be obscured. As for sample contact efficiency, pressure is essential for forcing the material to come into contact with the ATR crystal. This pressure is achieved with a sample holder that firmly presses the sample down. The stiffer materials, with curing speeds of either 100 or 1000 mm/min, resist fracture when compressed like this, but the softer materials crumble and spread. Not only are the softer materials more tightly pressed to the surface, the material in the crushed state covers more area of the ATR crystal. In addition, this crushing of the sample could have disrupted the gradient in cured material, and could have mixed the more cured material on the top

of the printed line with the less cured material on the bottom. These factors, the area of the crystal covered and the efficiency of contact, are likely to have affected the data, but exactly how remains uncertain.

In order to produce spectra that are smooth, some amount of filtering had to be used. This was accomplished using Savitzky-Golay filtering. The function requires both an order and a frame length. The output is a smooth spectrum, but this comes at the cost of either lost information or extraneous information being created. With this type of filtering, information is mostly just lost, as different peaks are merged together with higher smoothing. The DC calculated is very dependent on the values for the order and frame length, since it greatly affects the relative heights of the peaks, and might sometimes add peaks together that should, in reality, be separate. The effect of this could be limited if it could be determined what the ideal level of smoothing is for data such as these.

Conclusion

This work set out to determine the relationship between UV curing, time of irradiation, and thickness into the material. A 3D printer was used to extrude a methacrylate-based material onto the printer bed and was cured using a UV lamp. Using FTIR, the DC of the material was calculated. In running FTIR, several hundred spectra were obtained. Using MATLAB, these spectra were analyzed to obtain the ratio between peaks affected by the curing process and those unaffected.

These data collected in the experiment show that the DC of the material tends to decrease as the printing speed increases. Unfortunately, the variance in this data is far too high for any strict relationship to be quantified. This variance in the data could have been due to either errors in data analysis in MATLAB or due to errors in sample loading for FTIR.

Due primarily to the coronavirus pandemic, further data collection for this investigation has not been possible. This project, if it were to be finished, will require a significant amount of time and effort to collect and analyze the data necessary. Before doing this, however, work needs to be done investigating why exactly the data presented here have such high variability. If that can be done, the curing of the material could actually be investigated at multiple thicknesses as intended. Beyond the project presented here, future work could investigate the relationship between the materials' DC and its physical properties, especially mechanical properties such as

strength. The DC could also be investigated for printed material that uses different classes of material for the solids.

This work was supported by DTRA grant number HDTRA1-18-1-0004.

References

- [1] Brauer, G. M. (1978). Properties of sealants containing Bis-GMA and various diluents. *Journal of dental research*, 57(4), 597-607.
doi:<https://doi.org/10.1177/00220345780570041101>
- [2] Kalachandra S. , Taylor D.F., DePorter C.D. , Grubbs H.J. , McGrath J.E. (1993). Polymeric materials for composite matrices in biological environments. *Polymer*, 34(4): 778-782.
doi:[https://doi.org/10.1016/0032-3861\(93\)90363-F](https://doi.org/10.1016/0032-3861(93)90363-F)
- [3] Cramer, N. B., Stansbury, J. W., & Bowman, C. N. (2011). Recent advances and developments in composite dental restorative materials. *Journal of dental research*, 90(4), 402–416. doi: <https://doi.org/10.1177/0022034510381263>
- [4] Dickens S.H. , Stansbury J.W. , Choi K.M. , Floyd C.J.E. (2003). Photopolymerization Kinetics of Methacrylate Dental Resins. *Macromolecules*, 36(16):6043-6053.
doi:<https://doi.org/10.1021/ma021675k>
- [5] Al-Ahdal K. , Ilie N. , Silikas N. , Watts D.C. (2015). Polymerization Kinetics and Impact of Post Polymerization on the Degree of Conversion of Bulk-Fill Resin-Composite at Clinically Relevant Depth. *Dental Materials*, 31(10): 1207-1213.
doi:<https://doi.org/10.1016/j.dental.2015.07.004>
- [6] Czasch P. , Ilie N. (2013). In Vitro Comparison of Mechanical Properties and Degree of Cure of Bulk Fill Composites. *Clinical Oral Investigations*, 17(1): 227-235.
doi:<https://doi.org/10.1007/s00784-012-0702-8>
- [7] Eliades G.C. , Vougiouklakis G.J. , Caputo A.A. (1987). Degree of Double Bond Conversion in Light-Cured Composites. *Dental Materials*, 3(1): 19-25.
doi:[https://doi.org/10.1016/S0109-5641\(87\)80055-6](https://doi.org/10.1016/S0109-5641(87)80055-6)
- [8] Gonçalves, F. , Kawano, Y. , Pfeifer, C. , Stansbury, J. W. and Braga, R. R. (2009). Influence of BisGMA, TEGDMA, and BisEMA contents on viscosity, conversion, and flexural strength of experimental resins and composites. *European Journal of Oral Sciences*, 117: 442-446. doi:10.1111/j.1600-0722.2009.00636.x
- [9] Khan N. , Puntambeker S. (2017, Q2). Using Fourier Transform Infrared Spectroscopy for Development and Quality Assurance of Cure Chemistries. *Converting Quarterly*, 26, 68-73.
- [10] Knežević A. , Tarle Z. , Meniga A. , Šutalo, J. , Pichler G. , Ristić M. (2001). Degree of Conversion and Temperature Rise During Polymerization of Composite Resin Samples With Blue Diodes. *Journal of Dental Rehabilitation*, 28(6): 586-591.
doi:<https://doi.org/10.1046/j.1365-2842.2001.00709.x>
- [11] Lovell L.G. , Berchtold K.A. , Elliot J.E. , Lu H. , Bowman C.N. (2001). Understanding the Kinetics and Network Formation of Dimethacrylate Dental Resins. *Polym. Adv. Technol.* 12: 335-345. doi:<https://doi.org/10.1002/pat.115>

- [12] Ruiz, C.S.B. , Machado L.D.B. , Pino E.S. , Sampa M.H.O. (2002). Characterization of a Clear Coating Cured by UV/EB Radiation. *Radiation of Physics and Chemistry*, 63(3): 481-483. doi:[https://doi.org/10.1016/S0969-806X\(01\)00592-8](https://doi.org/10.1016/S0969-806X(01)00592-8)
- [13] Silikas N. , Eliades G. , Watts D.C. (2000). Light Intensity Effects on Resin-Composite Degree of Conversion and Shrinkage Strain. *Dental Materials*, 16(4): 292-296. doi:[https://doi.org/10.1016/S0109-5641\(00\)00020-8](https://doi.org/10.1016/S0109-5641(00)00020-8)
- [14] Ruiz, C. , Machado, L. , Vanin J. , Volponi, J. (2002). Cure Degree Estimation Of Photocurable Coatings by DSC and Differential Photocalorimetry. *Journal of Thermal Analysis and Calorimetry*, 67:335. doi:<https://doi.org/10.1023/A:1013914813678>
- [15] Yanyan, T. (2002) . *Stereolithography(SL) for Cure Modeling* (Master's Thesis). Retrieved from <https://smartechnology.gatech.edu/handle/1853/10143>
- [16] How deep does the infrared light penetrate at the position of contact between the prism and sample during ATR measurements? (n.d.). Retrieved October 18, 2019, from <https://www.shimadzu.com/an/ftir/support/faq/2.html>.
- [17] Gill P. , Moghadam T. T. , Ranjbar B. (2010). Differential Scanning Calorimetry Techniques: Applications in Biology and Nanoscience. *Journal of Biomedical Technology*, 21(4):167-193.
- [18] Ors J.A. , Scarlata S.F. (1985). *U.S. Patent No. 4651011*. Washington DC: U.S. Patent and Trademark Office.
- [19] Wang F.W. , Lowry R.E. Lin K. (1995). *U.S. Patent No. 5598005*. Washington DC: U.S. Patent and Trademark Office.
- [20] Woods H., Boddorff A., Ewaldz E, Adams Z, Ketcham M., Jang D.J., Sinner E., Thadhani E., Brettmann B. (2020). Rheological considerations for binder development in direct ink writing of energetic materials. *Propellants, Explosives, Pyrotechnics*. 45(26).

Appendix A – GCODE

```
M203 X8000 Y8000 Z1000 ;set the G0 speeds to slow
G21 ; set units to millimeters
G90 ; absolute coordinates
G53; Turn offsets off before homing.
G28 X0 Y0 ; home X and Y

;1-----
M221 T11 S1 P30 W1.6 Z1 ; set flow conditions
M674 T11 S2.0; turn on turbo mode
T0
G54 X0 Y0 Z0
M722 S10000 E5000 P1000 T11 I1 ; prime 5000 steps
G4 S.5
M722 S10000 E300 P100 T11 ; reset prime so doesn't double

G0 X375 Y90 ;move to starting pos
G1 Z1 F600 ;set layer height to lmm
G1 X175 Y90 F600 E1 ; print first start line
G1 X175 Y100 F600 E1 ; jog down
G1 X375 Y100 F600 E1 ; complete second start line
G1 X375 Y130 F600 E1; jog down
G1 X275 Y130 F600 E1
G1 X275 Y280 F600 E1

G0 Z10 ; move head up
G0 Z50 X500 ; move head out of way
M721 S10000 E5000 P500 T11 I1 ; unprime 10000 steps
G4 S.5 ; pause for unprime

M0 ; pause to put cap on

G0 X0 Y0
M620 E1.0 T13 ;enable laser
M621 T13 P100 ;set laser power in vector mode
T2
G1 Z9 E1 F1800 ;

G54 X69 Y15 Z9 ; set offset
G0 X375 Y90 Z1 ; go to starting position at 10mm Z
G1 X175 Y90 F2000 E1 ; print first start line
G1 X175 Y100 F2000 E1 ; jog down
G1 X375 Y100 F2000 E1 ; complete second start line
G1 X375 Y130 F2000 E1; jog down
G1 X275 Y130 F2000 E1;

;----- G1
X275 Y280 F100 E1; Change This one!!! ;-----
-----

M106 S0 T13 ; turn off light
T0 ; switch back to first head
```

```

G53
G0 Z10 ; move head up
G0 Z50 X500 ; move head out of way

M0 ; pause to clean up printer bed and collect sample

;2----- M221
T11 S1 P30 W1.6 Z1 ; set flow conditions
M674 T11 S2.0; turn on turbo mode
T0
G54 X0 Y0 Z0
M722 S10000 E5000 P1000 T11 I1 ; prime 5000 steps
G4 S.5
M722 S10000 E300 P100 T11 ; reset prime so doesn't double

G0 X375 Y90 ;move to starting pos
G1 Z1 F600 ;set layer height to 1mm
G1 X175 Y90 F600 E1 ; print first start line
G1 X175 Y100 F600 E1 ; jog down
G1 X375 Y100 F600 E1 ; complete second start line
G1 X375 Y130 F600 E1; jog down
G1 X275 Y130 F600 E1
G1 X275 Y280 F600 E1

G0 Z10 ; move head up
G0 Z50 X500 ; move head out of way
M721 S10000 E5000 P500 T11 I1 ; unprime 10000 steps
G4 S.5 ; pause for unprime

M0 ; pause to put cap on

G0 X0 Y0
M620 E1.0 T13 ;enable laser
M621 T13 P100 ;set laser power in vector mode
T2
G1 Z9 E1 F1800 ;

G54 X69 Y15 Z9 ; set offset
G0 X375 Y90 Z1 ; go to starting position at 10mm Z
G1 X175 Y90 F2000 E1 ; print first start line
G1 X175 Y100 F2000 E1 ; jog down
G1 X375 Y100 F2000 E1 ; complete second start line
G1 X375 Y130 F2000 E1; jog down
G1 X275 Y130 F2000 E1;

;----- G1
X275 Y280 F1000 E1; Change This one!!!
;-----

M106 S0 T13 ; turn off light
T0 ; switch back to first head
G53
G0 Z10 ; move head up
G0 Z50 X500 ; move head out of way

```

```

M0 ; pause to clean up printer bed and collect sample
;3-----
M221 T11 S1 P30 W1.6 Z1 ; set flow conditions
M674 T11 S2.0; turn on turbo mode
T0
G54 X0 Y0 Z0
M722 S10000 E5000 P1000 T11 I1 ; prime 5000 steps
G4 S.5
M722 S10000 E300 P100 T11 ; reset prime so doesn't double

```

```

G0 X375 Y90 ;move to starting pos
G1 Z1 F600 ;set layer height to 1mm
G1 X175 Y90 F600 E1 ; print first start line
G1 X175 Y100 F600 E1 ; jog down
G1 X375 Y100 F600 E1 ; complete second start line
G1 X375 Y130 F600 E1; jog down
G1 X275 Y130 F600 E1
G1 X275 Y280 F600 E1

```

```

G0 Z10 ; move head up
G0 Z50 X500 ; move head out of way
M721 S10000 E5000 P500 T11 I1 ; unprime 10000 steps
G4 S.5 ; pause for unprime

```

```

M0 ; pause to put cap on

```

```

G0 X0 Y0
M620 E1.0 T13 ;enable laser
M621 T13 P100 ;set laser power in vector mode
T2
G1 Z9 E1 F1800 ;

```

```

G54 X69 Y15 Z9 ; set offset
G0 X375 Y90 Z1 ; go to starting position at 10mm Z
G1 X175 Y90 F2000 E1 ; print first start line
G1 X175 Y100 F2000 E1 ; jog down
G1 X375 Y100 F2000 E1 ; complete second start line
G1 X375 Y130 F2000 E1; jog down
G1 X275 Y130 F2000 E1;

```

```

;----- G1
X275 Y280 F5000 E1; Change This one!!!
;-----

```

```

M106 S0 T13 ; turn off light
T0 ; switch back to first head
G53
G0 Z10 ; move head up
G0 Z50 X500 ; move head out of way
M0 ; pause to clean up printer bed and collect sample
;4-----
M221 T11 S1 P30 W1.6 Z1 ; set flow conditions
M674 T11 S2.0; turn on turbo mode
T0
G54 X0 Y0 Z0
M722 S10000 E5000 P1000 T11 I1 ; prime 5000 steps
G4 S.5

```

```

M722 S10000 E300 P100 T11 ; reset prime so doesn't double

G0 X375 Y90 ;move to starting pos
G1 Z1 F600 ;set layer height to 1mm
G1 X175 Y90 F600 E1 ; print first start line
G1 X175 Y100 F600 E1 ; jog down
G1 X375 Y100 F600 E1 ; complete second start line
G1 X375 Y130 F600 E1; jog down
G1 X275 Y130 F600 E1
G1 X275 Y280 F600 E1

G0 Z10 ; move head up
G0 Z50 X500 ; move head out of way
M721 S10000 E5000 P500 T11 I1 ; unprime 10000 steps
G4 S.5 ; pause for unprime

M0 ; pause to put cap on

G0 X0 Y0
M620 E1.0 T13 ;enable laser
M621 T13 P100 ;set laser power in vector mode
T2
G1 Z9 E1 F1800 ;

G54 X69 Y15 Z9 ; set offset
G0 X375 Y90 Z1 ; go to starting position at 10mm Z
G1 X175 Y90 F2000 E1 ; print first start line
G1 X175 Y100 F2000 E1 ; jog down
G1 X375 Y100 F2000 E1 ; complete second start line
G1 X375 Y130 F2000 E1; jog down
G1 X275 Y130 F2000 E1;

;----- G1
X275 Y280 F7500 E1; Change This one!!!
;-----

M106 S0 T13 ; turn off light
T0 ; switch back to first head
G53
G0 Z10 ; move head up
G0 Z50 X500 ; move head out of way
M0 ; pause to clean up printer bed and collect sample
;5-----
M221 T11 S1 P30 W1.6 Z1 ; set flow conditions
M674 T11 S2.0; turn on turbo mode
T0
G54 X0 Y0 Z0
M722 S10000 E5000 P1000 T11 I1 ; prime 5000 steps
G4 S.5
M722 S10000 E300 P100 T11 ; reset prime so doesn't double

G0 X375 Y90 ;move to starting pos
G1 Z1 F600 ;set layer height to 1mm
G1 X175 Y90 F600 E1 ; print first start line
G1 X175 Y100 F600 E1 ; jog down
G1 X375 Y100 F600 E1 ; complete second start line
G1 X375 Y130 F600 E1; jog down

```

```

G1 X275 Y130 F600 E1
G1 X275 Y280 F600 E1

G0 Z10 ; move head up
G0 Z50 X500 ; move head out of way
M721 S10000 E5000 P500 T11 I1 ; unprime 10000 steps
G4 S.5 ; pause for unprime

M0 ; pause to put cap on

G0 X0 Y0
M620 E1.0 T13 ;enable laser
M621 T13 P100 ;set laser power in vector mode
T2
G1 Z9 E1 F1800 ;

G54 X69 Y15 Z9 ; set offset
G0 X375 Y90 Z1 ; go to starting position at 10mm Z
G1 X175 Y90 F2000 E1 ; print first start line
G1 X175 Y100 F2000 E1 ; jog down
G1 X375 Y100 F2000 E1 ; complete second start line
G1 X375 Y130 F2000 E1; jog down
G1 X275 Y130 F2000 E1;

;-----
G1 X275 Y280 F10000 E1; Change This one!!!
;-----
M106 S0 T13 ; turn off light
T0 ; switch back to first head
G53
G0 Z10 ; move head up
G0 Z50 X500 ; move head out of way M30
; End Program

```

Appendix B – MATLAB Code

```

function [data,curingA,curingP] = IRanalysis(Name,Date,startAt,dim,varargin)
%name is the part of the file that is unique to this batch of data\
%date is the date the data were collected on
%startat is the number corresponding to the letter of the sample that the
%data start at
%ex. ZA1-51G -> startAt=7
%dim is the dimensions the data should be in:
% dim(1) 'm' - total number of samples (vertical dimension)
% dim(2) 'n' - number of runs per sample (horizontal dimension)
%varargin allows for felxible number of inputs

%Default State of Program,
%-----
graphData=false; loadData=true; normData=true; meanData=false; curingP=[];
curingA=[]; names=[]; frame = 51; order=4;
points={ [1653,1623,1592,1565]};
%-----
%Applying variable inputs [~,i]=size(varargin);
for x = 1:i      if floor(x/2)~=x      if
~iscell(varargin{1,x})      switch
varargin{1,x}      case 'Graph'
graphData = varargin{1,x+1};
case 'Load'      loadData =
varargin{1,x+1};      case 'Norm'
normData = varargin{1,x+1};
case 'Mean'      meanData =
varargin{1,x+1};      case 'Names'
names=varargin{1,x+1};      case
'Points'      points =
varargin{1,x+1};      case 'P'
P=varargin{1,x+1};
case 'Order'
order=varargin{1,x+1};      end
end      end end
%Data Loading
%-----
%Program checks if data is saved to workspace. If not it manually loads
%data from .txt files
letters=char(64+startAt:90); data = cell(dim(1),dim(2)); if
exist([Date, '.mat'])==2      load([Date, '.mat']); else      for y=1:dim(1)
for x=1:dim(2)      try      path
=sprintf('/Users/Zadams/Desktop/Everything For Thesis/FTIR/%s/%s%-
%s.txt',Date,Name,letters(y),num2str(x));      fID = fopen(path);
if fID==-1      path
=sprintf('/Users/Zadams/Desktop/Everything For Thesis/FTIR/%s/%s%-
%s.txt',Date,Name,letters(y),num2str(x));
fID=fopen(path);      end      fgetl(fID);
catch      error('IRanalysis:badDim','Dimension mismatch.\nCheck
to make sure the entered dimensions are correct');      end
data{y,x}=transpose(fscanf(fID,'%f %f',[2 Inf]));      end      end
save(Date,'data'); end
%----- Filtering -----% for y=1:size(data,1)      for
x=1:size(data,2)

```

```

data{y,x}=[data{y,x}(:,1),sgolayfilt(data{y,x}(:,2),3,31)];
end end
%-----
%-----Data Analysis-----
%-----
X = data{1,1}(:,1); yy1=cell(dim(1),dim(2)); yy2=yy1; cure=yy1; cureP=yy1;
DataAdj=data; for y=1:dim(1) for x=1:dim(2)
    %--- Normalizing data by area -----%
    Area=cumtrapz(data{y,x}(:,1),data{y,x}(:,2));
AreaAdj = Area./Area(finder(X,1720));
specAdj = Diff([X,AreaAdj]); specAdj =
specAdj(:,2);
specAdj2=specAdj./specAdj(finder(X,1720));
DataAdj{y,x}=[X,specAdj2];

    if size(points,1)>1
p=points{y,x}; else
p=points{1,1}; end
    ndxPTS=[finder(X,p(4)),finder(X,p(3)),finder(X,p(2)),finder(X,p(1))];
xs =
[X(finder(X,p(4))),X(finder(X,p(3))),X(finder(X,p(2))),X(finder(X,p(1)))]];
A = DataAdj{y,x}(:,2); mask12 = and(X>=xs(1),X<=xs(2));
%----- Slope -----%
slope1=(A(X==xs(4),1)-A(X==xs(2),1))/(xs(4)-xs(2));
slope2=(A(ndxPTS(2),1)-A(ndxPTS(1),1))/(X(ndxPTS(2))-X(ndxPTS(1)));
%----- Baseline -----%
yy1{y,x}=slope1.*(X(mask24)-xs(4))+A(ndxPTS(4),1);
yy2{y,x}=slope2.*(X(ndxPTS(1):ndxPTS(2))-
X(ndxPTS(2))+A(ndxPTS(2),1);
%----- Peak Finding -----%
A1 = [A(mask12)-yy2{y,x};A(mask24)-yy1{y,x}];
X1 = [X(mask12);X(mask24)];
[pks,locs,~,~]=findpeaks(A1);% find peaks of data
[~,locs2,~,~]=findpeaks(-A1);%find troughs of data m1
=
[and(locs>=P{1}(1),locs<=P{1}(2)),and(locs>=P{2}(1),locs<=P{2}(2))]; %turn
peaks into a mask to access the rest of the data m2 =
[and(locs2>=P{3}(1),locs2<=P{3}(2)),and(locs2>=P{4}(1),locs2<=P{4}(2))];
z=zeros(length(m2(m2(:,2),2)),1);%-----
[~,e]=max(pks(m2(:,2))); %| z(e)=1;
%| m2(m2(:,2),2)=z; %| This is done to
ensure there is only one peak z=zeros(length(m2(m2(:,1),1)),1);
%| at the spot I want
[~,e]=max(pks(m2(:,1))); %|
z(e)=1; %|
m2(m2(:,1),1)=z; %----- mx1
= and(X1>=X1(1),X1<=X1(locs2(m2(:,1))))); mx2 =
and(X1>=X1(locs2(m2(:,2))),X1<=X1(end));
%----- Integrating -----%
a1 = trapz(X1(mx1),A1(mx1));
a2= trapz(X1(mx2),A1(mx2));
%----- Peak Heights -----%
p1=pks(m1(:,1));
p2=pks(m1(:,2));

```

```

        cure{y,x}=[a2;a1];
cureP{y,x}=[p2;p1];
end end curingA=cure;
curingP=cureP;

%-----
%-----Graphing-----
%-----
if graphData      graphs=Graph(DataAdj2);      if ~isempty(names)
legend(graphs,names,'location','southwest');      end end fclose('all');
end function index =
finder(x,target)
%finder(X,1620) -> the closest index to 1620cm^-1
spacing = mean(diff(x));
U = target+(spacing/2);
L=target-spacing/2; index =
find(and(x<=U,x>=L)); end
function outGraph = Graph(dataIn)
[m,n]=size(dataIn); l=m;
color1 = [69, 255, 41]/255;
color2 = [2, 1, 77]/255;
colors = [linspace(color1(1),color2(1),l)', linspace(color1(2),color2(2),l)',
linspace(color1(3),color2(3),l)'];
figure('Renderer', 'painters', 'Position', [10 10 900 600])
hold on outGraph=gca; for y=1:m      for x=1:n
outGraph(y,x)=plot(dataIn{y,x}(:,1),dataIn{y,x}(:,2), 'Color', colors(y,:))
;      end end
title({'FTIR Spectra of 61.4% hSiO2 in 2:1 BisGMA:TEGDMA','at 0.083mm/s
24h after irradiation'}); xlabel('Wavenumber [cm^-1]');
ylabel('Absorbance');
set(gca, 'XDir', 'reverse', 'xlim', [1550,1780], 'ylim', [-
0.01,1.05], 'FontSize',15);
plot([1608,1608], [-10,20], 'k:');
plot([1637,1637], [-10,20], 'k:');
plot([1582,1582], [-10,20], 'k:');
plot([1720,1720], [-10,20], 'k:');
plot([0,2000], [0,0], 'k--'); end
function outDiff = Diff(dataIn) h = mean(diff(dataIn(:,1)));
outDiff=zeros(size(dataIn)); outDiff(:,1)=dataIn(:,1); for
x=1:size(dataIn,1)      if and(x>2,x<size(dataIn,1)-2)      d = (-
dataIn(x+2,2)+8*dataIn(x+1,2)-8*dataIn(x-1,2)+dataIn(x-
2,2))./(12*h);
outDiff(x,2)=d;
end end end

```